

Studies on Single- and Dual-Wavelength DPR Retrievals: Algorithm Evaluation

Liang Liao
GESTAR/MSU, Greenbelt, MD

Robert Meneghini
NASA/GSFC, Greenbelt, MD

Ali Tokay
UMBC/JCET, Greenbelt, MD

Hyokyung Kim
GESTAR/MSU, Greenbelt, MD

Introduction

The current DPR-operational algorithm adopts an optimization approach that is based on a relationship between rain rate (R) and mass-weighted diameter (D_m), i.e., R- D_m relation. Constraint of the R- D_m relation leaves gamma DSD having only one free parameter, such as D_m , if its shape factor is either fixed or expressed as a function of D_m . Thus, one is able to relate the radar reflectivity to D_m . An adjustment factor is used to modify R- D_m relation for each vertical hydrometeor profile. A search for the adjustment factor is conducted by minimizing differences between simulated and measured radar reflectivities as well as the path integral attenuation (PIA) in the case of a single wavelength and differential PIA (δPIA) for dual-wavelengths. Once the adjustment factor is found, the DSD and R can be uniquely derived along each profile. An obvious advantage of this optimal approach is to avoid retrieval uncertainties arising from the double solutions such as those that occur from the use of the DFR. Its performance depends on a number of factors that include the model assumptions and the degree of uniformity of the DSD along the profiles. An evaluation of the algorithm performance is important in assessing the strengths and weaknesses of the algorithm and in gaining insight into the ways to improve it.

Simultaneous comparisons of co-located PR and DPR estimates with the similar quantities derived from the ground measurements provide direct checks of the PR/DPR algorithms. This is in fact a very important task for the validation of the DPR products. However, because of different beamwidths, scanning geometries and possible temporal offsets, the space- and ground-radar scattering volumes cannot be perfectly matched. In addition, the issue of non-uniform beam filling (NUBF) further complicates the algorithm evaluation. While direct comparisons between space- and ground-based sensors remain essential, they do not fully meet the need for algorithm testing and improvement. To validate the algorithm principles and their assumptions, a physical and realistic framework/test-bed is employed to enable an accurate assessment of the performance of the algorithms.

To achieve this, measured time-series DSD data are used to construct vertical rain profiles. With the known profile of particle size distribution, the true and measured reflectivity factors as well as path integral attenuation (PIA) can be computed from forward scattering models. The Ku- and Ka-band measured reflectivity profiles can then be used as input to the retrieval algorithms. The degree to which the radar estimates agree with the true values, which are derived directly from the assumed DSD profiles, constitutes a measure of the retrieval accuracy. The basic approach can also be used to evaluate the impact of different model assumptions and various constraints adopted in the retrieval algorithms.

Seto, S., T. Iguchi and T. Oki, 2013: The basic performance of a precipitation retrieval algorithm for the Global Precipitation Measurement mission's single/dual frequency radar measurements. *IEEE Trans. Geosci. Remote Sens.*, 51, 5239-5251.
Seto, S., and T. Iguchi, 2015: Intercomparison of attenuation correction methods for the GPM dual-frequency precipitation radar. *J. Atmos. Oceanic Technol.*, 32, 915-926.

DPR Algorithms

From R- D_m relation expressed as $R = \varepsilon^\tau a D_m^b$ (1)

From Look-up tables $R = N_w I_R(D_m, \mu)$ (2)

Then, we have $N_w = \frac{R}{I_R(D_m, \mu)} = \frac{\varepsilon_k^\tau a D_m^b}{I_R(D_m, \mu)}$ (3)

And also, $Z_e = 10 \text{Log}_{10}(N_w) + I_b(D_m, \mu)$

Substituting (3) into above equation, we obtain

$$Z_e = 10 \text{Log}_{10}(\varepsilon_k^\tau a) + 10b \text{Log}_{10} D_m - 10 \text{Log}_{10} I_R(D_m, \mu) + I_b(D_m, \mu) \quad (4)$$

D_m could uniquely be solved from Eq.(4). Once D_m is determined, R and N_w are obtained from Eq.(1) and (3), respectively. From derived DSD parameters $Z(\lambda)$ and $k(\lambda)$ are then computed. ε is chosen so that

$$p_1(\varepsilon) p_2(\varepsilon) p_3(\varepsilon) = \max(p_1(\varepsilon_k) p_2(\varepsilon_k) p_3(\varepsilon_k), k = 1, 2, \dots, K)$$

$$p_1(\varepsilon) = \frac{1}{\sigma_1 \sqrt{2\pi}} \exp\left(-\frac{(\log \varepsilon)^2}{2\sigma_1^2}\right)$$

$$p_2(\varepsilon) = \frac{1}{\sqrt{2\pi}} \exp\left(-\frac{(\delta PIA - \delta PIA_{SRT})^2}{2\sigma_2^2}\right)$$

$$p_3(\varepsilon) = \prod_{i=1}^N \frac{1}{\sqrt{2\pi}} \exp\left(-\frac{(Z_{m,est}^{(Ka)} - Z_{m,lpbs}^{(Ka)})^2}{2\sigma_3^2}\right)$$

Algorithm Evaluation

1. Examples of profile retrievals

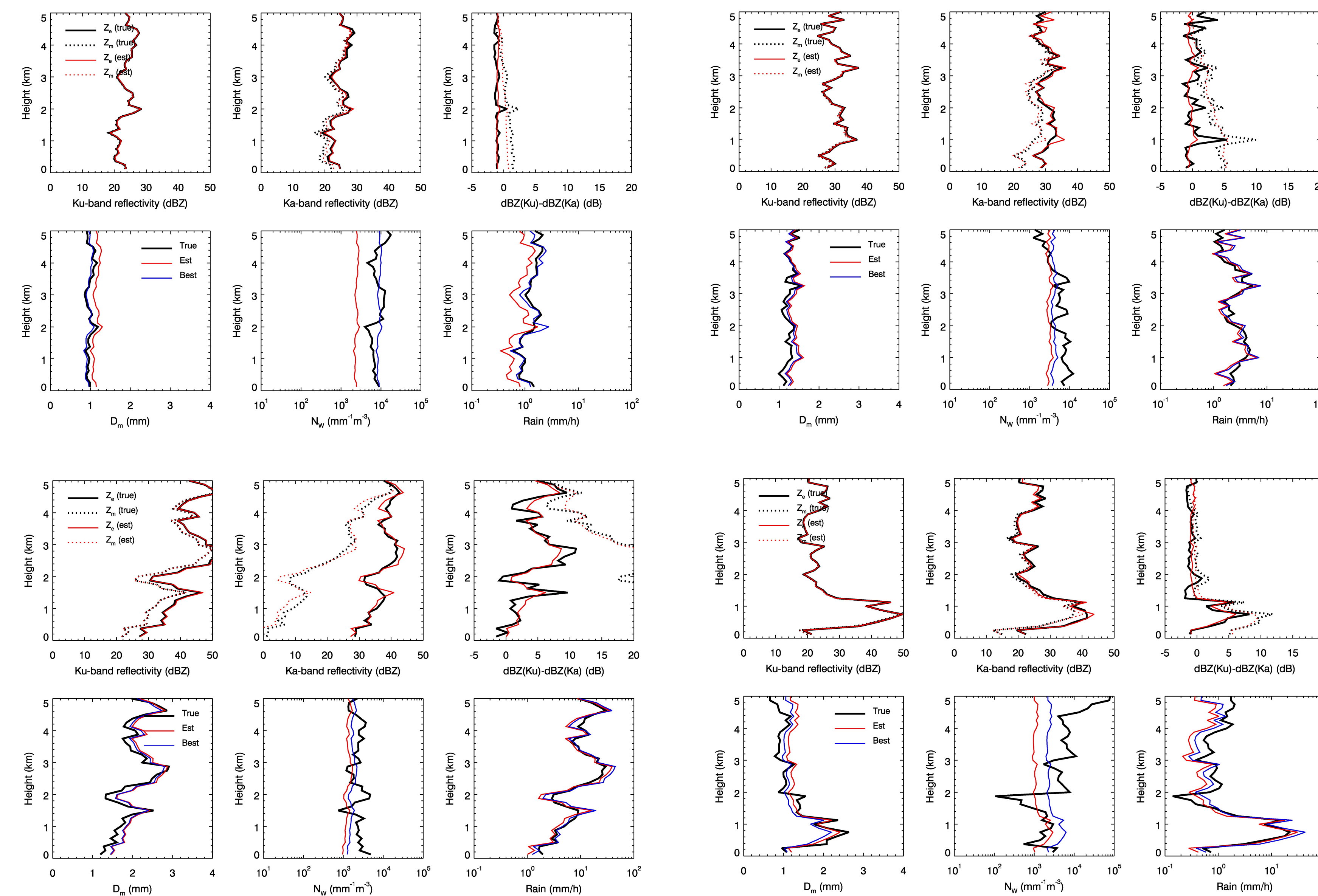


Fig.1 Comparisons of radar reflectivities, DSD and rainfall rate profiles between the DPR-estimated (red) and their true values (black). The results from 4 cases that correspond to light (top-left set of the plots), moderate (top-right), heavy (bottom-left) and high-degree non-uniform (bottom-right) rain are provided. For reference also given are the best solutions with respect to D_m and R in the solution space in which the solutions are arranged as a function of $\log_{10}(\varepsilon_k)$, $k=1,2,\dots,K$. In perfect conditions or under strong conditions the estimated solutions coincide with the best solutions. Weak constraints lead to departures of the estimated from the best solutions. The differences between the best and truth are largely due to imperfection of the models assumed, such as vertically constant R- D_m relation and DSD parameterizations.

2. Statistical comparisons

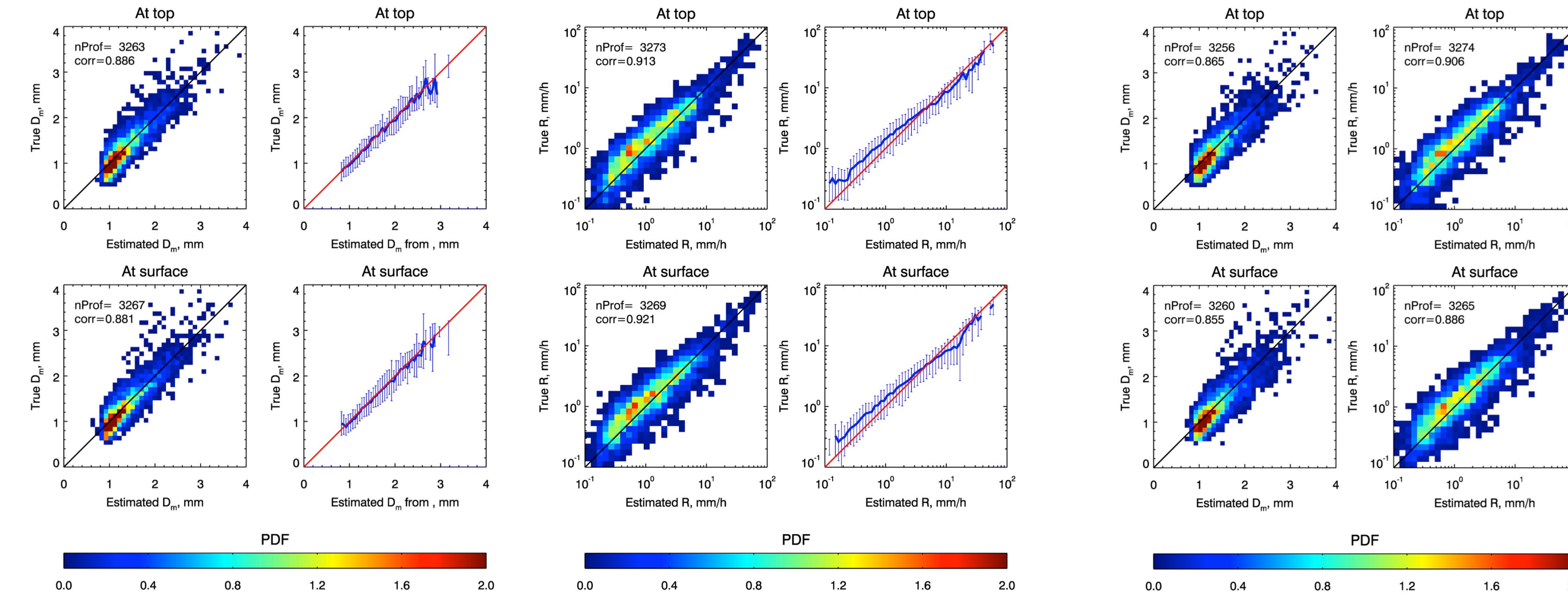


Fig.2 Comparisons of D_m (left panel) and R (right panel) estimated by the DPR dual-wavelength algorithm with their true values at the gates of rain top and surface as the forward recursive approaches are applied to non-uniform DSD profiles. The PDFs obtained from the data points of estimated and true values are shown in the left column of each panel while the means (thick blue curves) and the 2-time standard deviations (thin blue vertical bars) derived from the same data points are displayed in the right column. One-to-one relations (black and red lines) are also plotted for references.

Fig.3 PDFs of D_m (left column) and R (right column) estimated by the DPR dual-wavelength algorithm with the true rain rates at the gates of rain top (top row) and surface (bottom row) as the backward recursive approaches are applied to non-uniform DSD profiles.

Algorithm Evaluation (Cont'd)

3. Retrieval from various degrees of non-uniformity of hydrometeor profiles

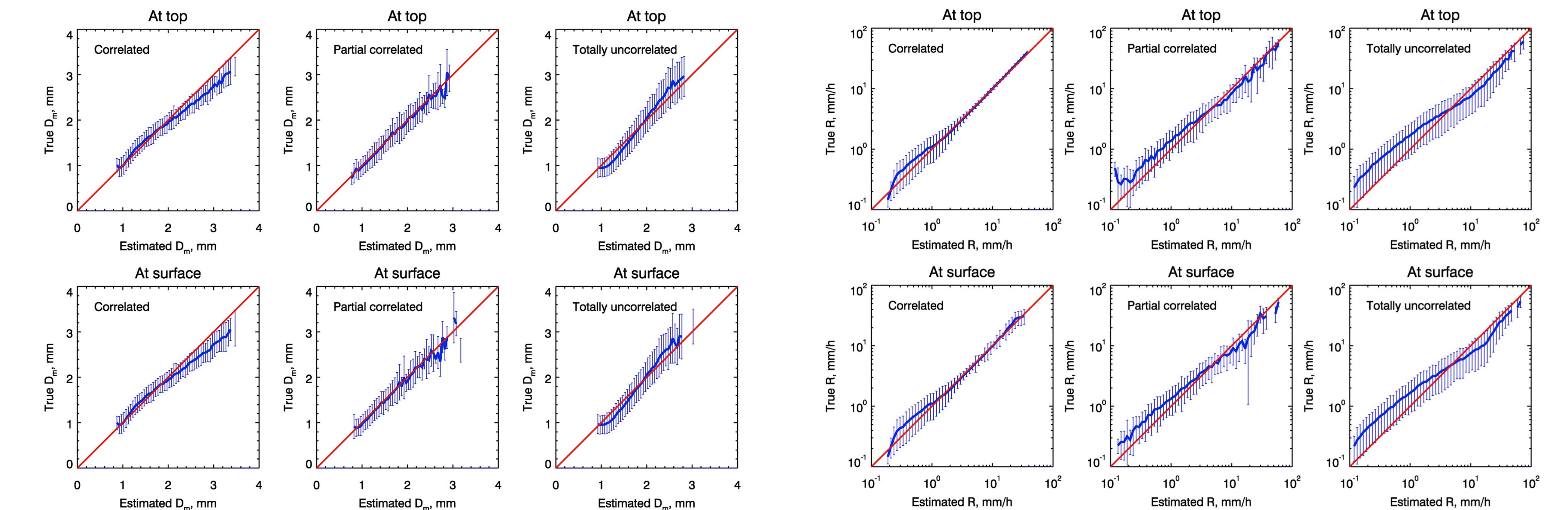


Fig.4 Comparisons of D_m (left panel) and R (right panel) estimated by the DPR dual-wavelength algorithm with truth at the gates of rain top (top row) and surface (bottom row) as the forward recursive approaches are applied to the fully-correlated (uniform), partially-correlated (non-uniform) and totally-uncorrelated (extremely non-uniform) vertical DSD profiles. The means (thick blue curves) and the 2-time square root of error variances (thin blue vertical bars) are computed from the data points of estimated and true values within intervals between D_m (R) and $D_m + \Delta D_m$ ($R + \Delta R$). An unbiased statistical δPIA model with the standard deviation of 0.8 dB is assumed. One-to-one relations (red lines) are also plotted for references.

4. Retrieval from different R- D_m relations

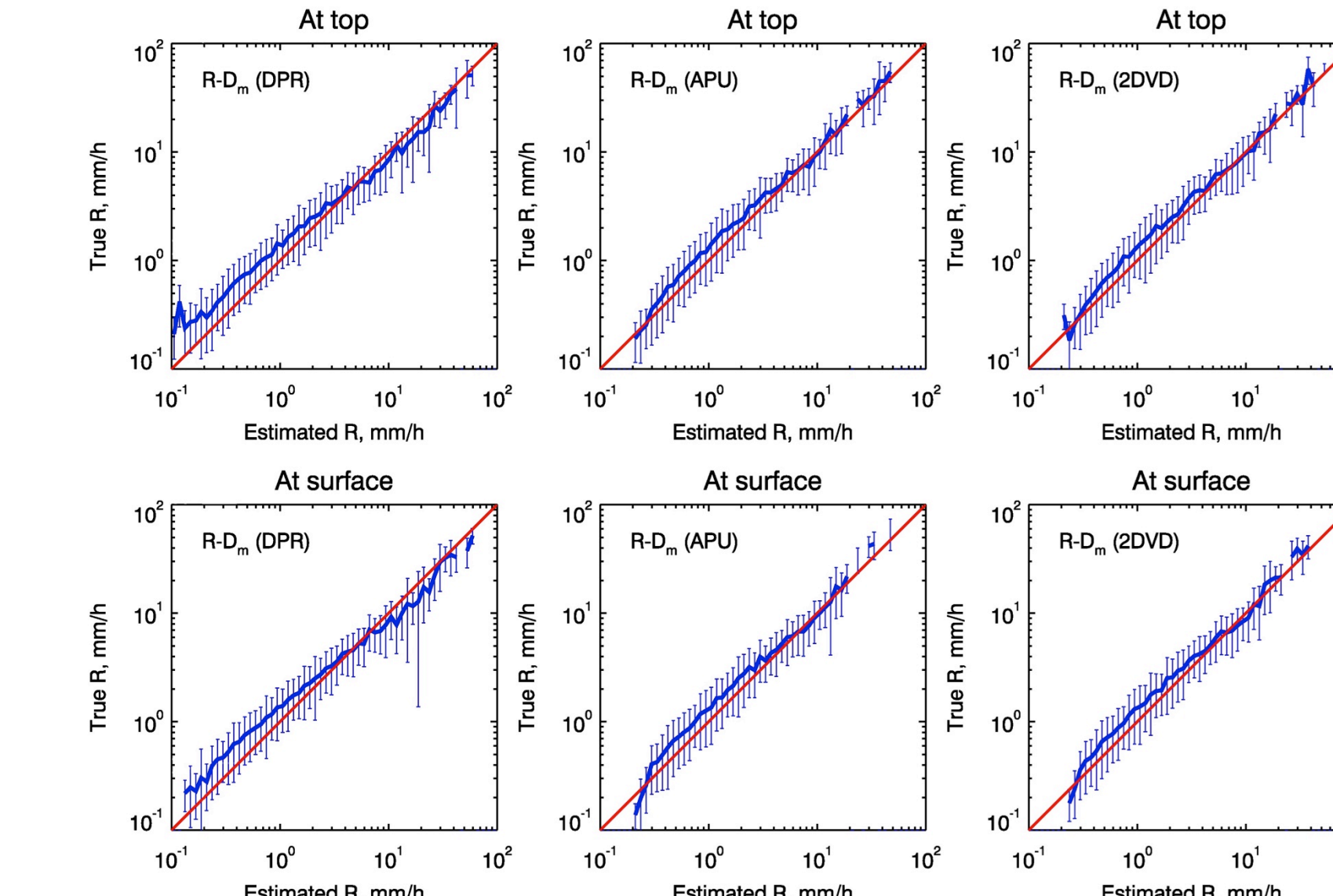


Fig.5 Comparisons of R estimated by the DPR dual-wavelength algorithm with DPR-default (left), Parsivel-DSD-derived (middle) and 2DVD-DSD-derived (right) R- D_m relations being used with true R as the forward recursive approaches are applied to the non-uniform vertical DSD profiles.

5. Roles of p_1 , p_2 and p_3 to retrieval

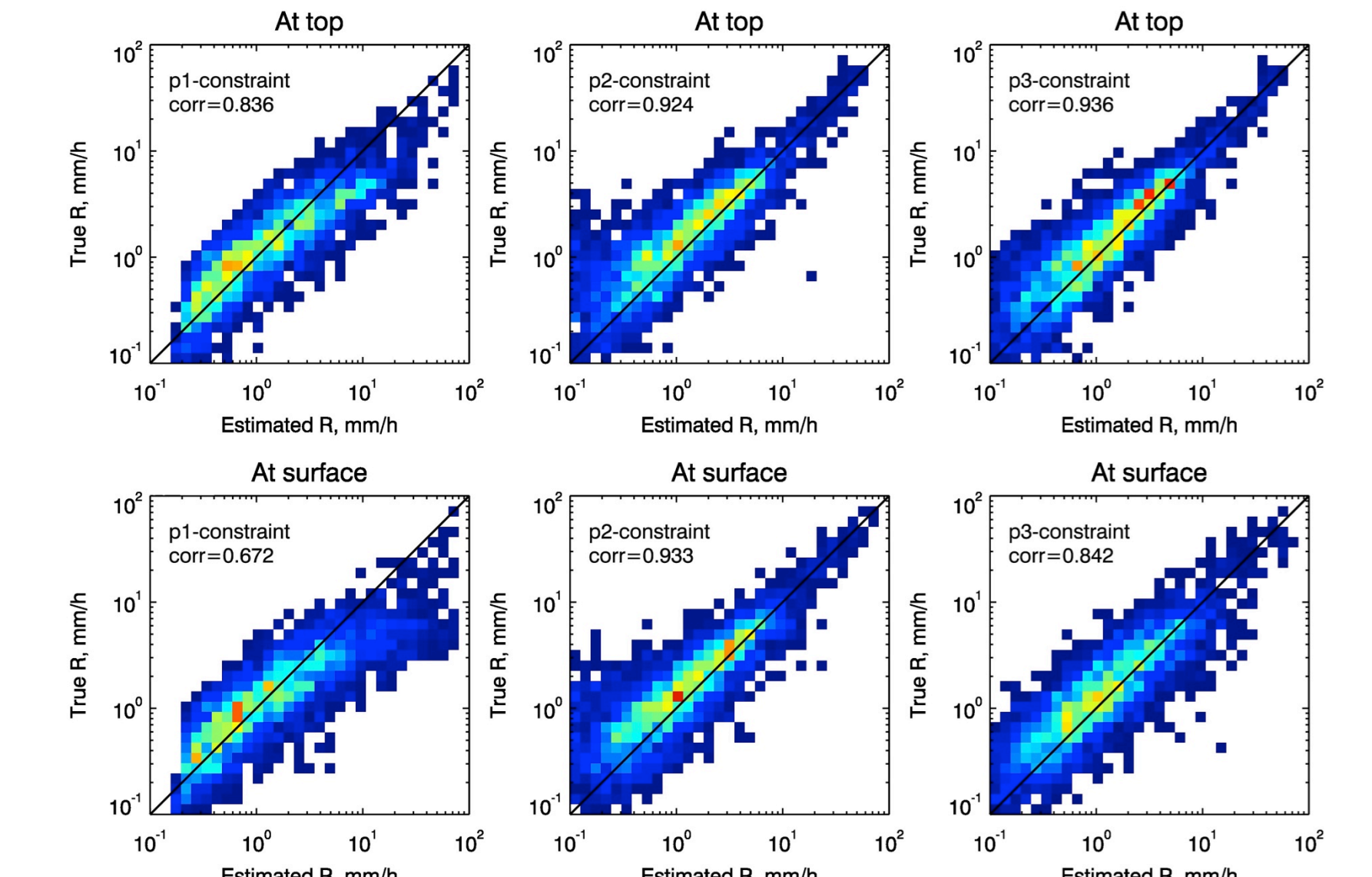


Fig.6 PDFs of R estimated by the DPR dual-wavelength algorithm and true rain rates as the algorithms employ only single individual constraints in selection of ε , such as p_1 (left column), p_2 (center column) and p_3 (right column).

6. Comparison of single- and dual-wavelength retrieval

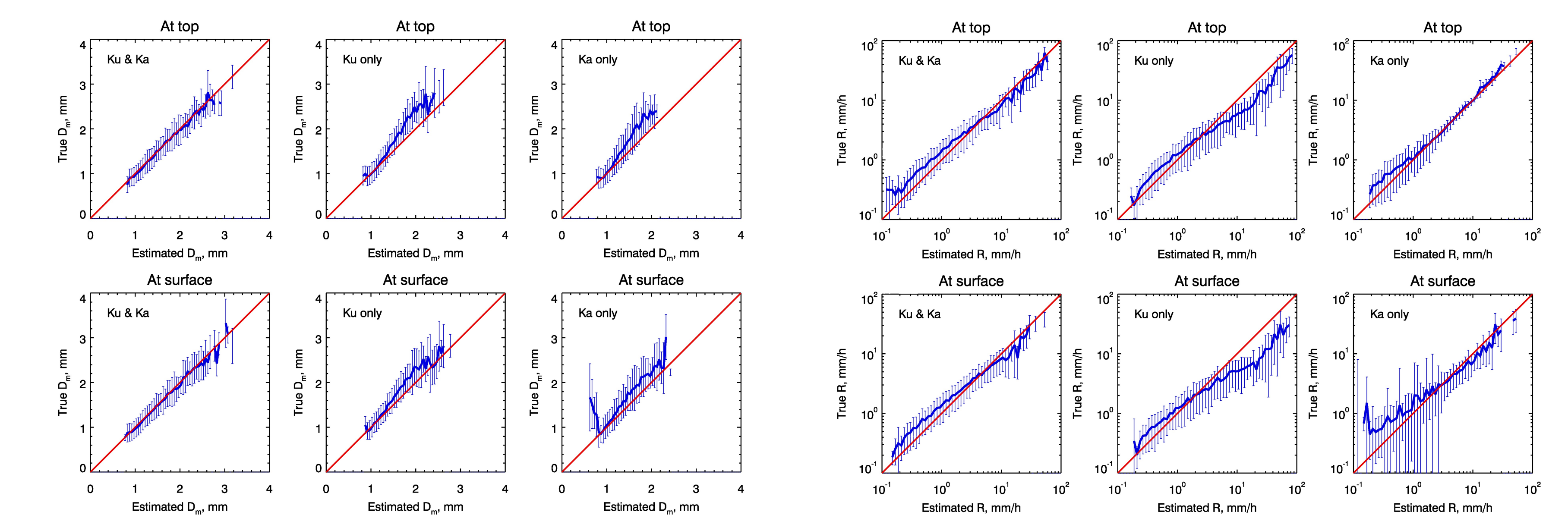


Fig.7 Comparisons of the DPR dual-wavelength and single-wavelength performances in estimating D_m (left) & R (right) as the DPR-like forward recursive approaches are applied to the non-uniform vertical DSD profiles. The means (thick blue curves) and the 2-time square root of error variances (thin blue vertical bars) are computed from the data points.